 doi: 10.1111/j.1365-246X.2006.02904.x

Distributed Nubia–Somalia relative motion and dike intrusion in the Main Ethiopian Rift

R. Bendick, S. McClusky, R. Bilham, L. Asfaw and S. Klemperer

Department of Geology, University of Montana, Missoula, MT 59812, *USA*

Accepted 2005 December 20. Received 2005 December 16; in original form 2005 March 18

SUMMARY

The Main Ethiopian Rift (MER) in central Ethiopia extended in the rift-normal direction at a mean rate of 4.0 ± 0.9 mm yr^{-1} (1σ) during the period 1992–2003, nearly a factor of two slower than the opening rate estimated from global plate motion inversions. Rift opening near a geodetic array during this period was accommodated by a single dike injection event in 1993, spatially coincident with active magmatic segments, probably triggered by observed seismicity. Following dike injection, the crust in the rift relaxed as a layered medium, with a ∼15-km-thick elastic lid over a viscous half space of 10^{18} Pa s. Diking, rather than normal faulting on rift-bounding faults, appears to be the predominant mechanism of extension in the MER, explaining the very low regional rates of moment release. The length scale and temporal behaviour of surface displacements require viscoelastic rheology in the rift.

Key words: African rift, continental rifting, geodesy, viscoelasticity.

INTRODUCTION

In this paper we interpret Global Positioning System (GPS) observations across the Main Ethiopian Rift (MER) between 1992 and 2003. These improve the temporal and spatial resolution of estimates of relative displacement between Nubia and Somalia in central Ethiopia. With improved resolution, we observe low mean rift opening rates, secular deceleration in rift opening from 1993 to 2003 and strain localization centred on a mid-rift magmatic segment rather than on rift-bounding normal faults.

The East African Rift (EAR) forms one axis of extension from a triple junction at the Afar depression; the other two arms are oceanic ridges presently producing sea floor in the Gulf of Aden and the Red Sea (Fig. 1). Miocene and Recent volcanism (Ebinger *et al.* 1993), seismic moment release (Kebede & Kulhanek 1991) and anomalously low S-wave velocities (Knox *et al.* 1999; Weeraratne *et al.* 2005), all indicate ongoing tectonic deformation in the Ethiopian segment of the EAR.

Rift-bounding faults in the MER demonstrate activity from 11 Ma (Woldegabriel *et al.* 1990; Wolfenden *et al.* 2004), with a change in the maximum extension direction from 130°E to 105°E between 6.6 and 3 Ma (Wolfenden *et al.* 2004). Several studies (e.g. Ebinger & Casey 2001; Kendall *et al.* 2005) indicate that Quaternary extension in the rift is accommodated at least partially by volcanism in mid-rift magmatic segments.

During the period 1963–2002, seismic moment of fewer than 3.69×10^{19} N m were released in the rift segment from the Kenyan border to the Red Sea (Kebede & Kulhanek 1991; Foster & Jackson 1998; Engdahl *et al.* 1998; Harvard CMT). These events were organized into two or three geographical clusters. The vast majority occurred within the Afar depression and the southern Ethiopian Rift (Fig. 1). Recorded seismic release near the geodetic array described here (Fig. 1) is limited to a large event in 1906 (estimated at ∼M6.8), a swarm of microseisms near Nazret in 1964, and an Mw = 5.3 event near Nazret in 1993 discussed in detail below (Fig. 2). Two additional swarms with maximum local magnitude of 4 occurred near Fantale and Dofen (Fig. 2) volcanoes in 1981 and 1989. A regional array of seismometers deployed in the MER in 2002–2003 recorded 173 local events located within 1° of the geodetic array (Keir *et al.* 2004, 2006), but the total moment released is only 3.03×10^{14} N m, the equivalent of one Mw = 3.6 event. Hofstetter & Beyth (2003) describe seismicity in this region as diffuse, with seismic efficiency (the ratio between the observed seismic moment and geologically/geodetically predicted moment) of <50 per cent, indicative of significant aseismic accommodation of tectonic strain.

Slip on faults appears to have slowed in favour of dike injection associated with magmatic segments in the past 1.8 Ma (Fig. 2) (Ebinger & Casey 2001; Wolfenden *et al.* 2004; Keranen *et al.* 2004). Acocella *et al.* (2003) document specific scaling relations for both tensile cracks and normal faults in the axial region of the MER. They observe that cracks are limited to lengths of <800 m and dilations of 2–4 m, after which they become normal faults and continue to grow. This fault morphology and surface dike geometry demonstrate that the present dominant mode of deformation in the MER is subsurface dike injection (Gloaguen *et al.* 2003; Wolfenden *et al.* 2005). Shear-wave polarization anisotropy within the MER gives a fast direction orthogonal to the modern ESE extension direction (Gashawbeza *et al.* 2004), interpreted by Kendall *et al.* (2005) as being due to the orientation of many dikes along the rift axis, though the greatest splitting is associated with the rift-bounding faults and the rift shoulder changes in crustal thickness.

3-D tomography from a controlled-source seismic experiment in 2003 shows large en-echelon intrusions corresponding to magmatic segments at depths of approximately 10 km (Keranen *et al.* 2004).

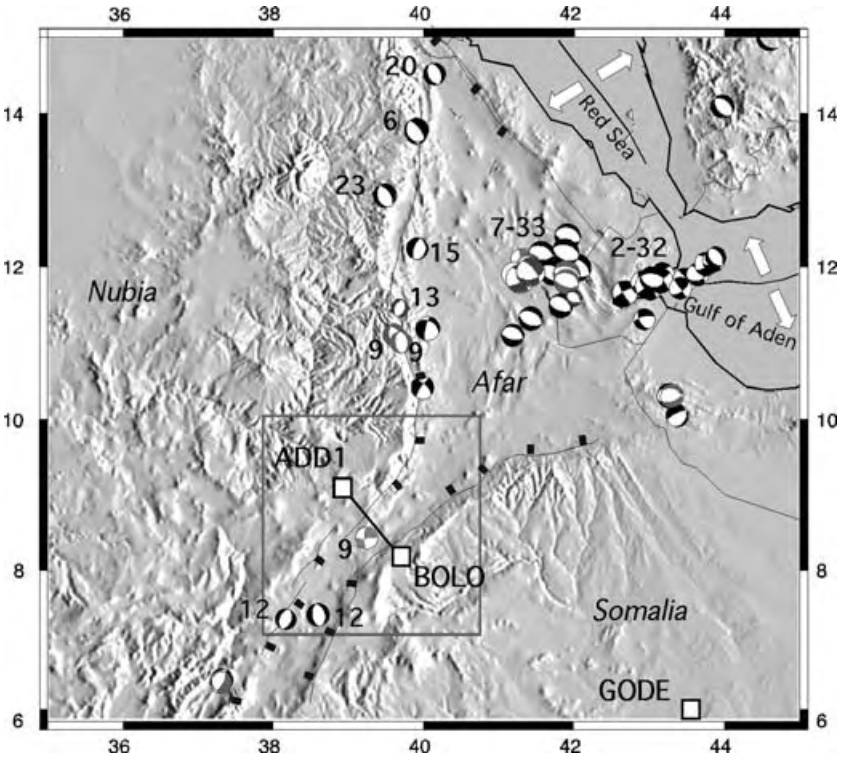

Figure 1. Regional tectonic and topographic setting of the Ethiopian Rift. Focal mechanisms in black are from the Harvard CMT catalogue, in grey are from Kebede & Kulhanek (1991), stippled are from Foster & Jackson (1998). The striped mechanism is the 1933 February 13 Mw = 5.3 event at its relocated epicentre. Numbers are relocated event depths from Engdahl *et al.* (1998), where available. The solid line marks the position of the geodetic array, and the grey square the location of Fig. 2.

The host material is interpreted as continental crust of lower seismic velocity, probably Precambrian crust, overlain by pre-rift flood basalts and subsequent extrusive igneous flows (Keranen *et al.* 2004; Maguire *et al.* 2006). The lower crust contains only modest amounts of intruded mafic material related to surface flood basalts and rift volcanism (Maguire *et al.* 2006) underlain by anomalously hot asthenosphere (Bastow *et al.* 2005). Crust heated by intrusions within the rift is weak, as suggested by gravity admittance inversions giving $Te = 8 \pm 2$ km (Ebinger & Hayward 1996). Hypocenter distribution suggests seismogenic thickness in the central MER is less than 10–15 km (Fig. 1), but the number of events with high-quality depth estimates (Engdahl *et al.* 1998) in the MER is small.

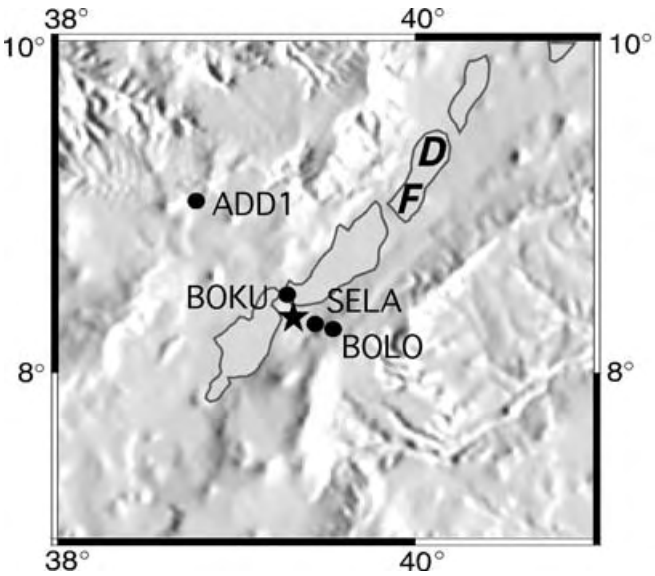

Figure 2. GPS sites are marked with points and station names. Magmatic segments (from Ebinger & Casey 2001) are stippled. The relocated epicentre of the 1993 right lateral earthquake is marked with a black star. Fantale and Dofen volcanoes are marked F and D, respectively. For discussion see text.

Estimates of relative velocity between Nubia and Somalia correlate to the length scale over which displacement is integrated (Fig. 3). Relative velocity calculated from far-field observations, particularly global plate-motion inversions (Fernandes *et al.* 2004; Sella *et al.* 2002) and magnetic anomalies on the Southwest Indian Ridge (Lemaux *et al.* 2002; Chu & Gordon 1999) yield MER opening rates from 6 mm a^{-1} (Chu & Gordon 1999) to 7.3 mm a^{-1} (Fernandes *et al.* 2004). The median opening rate from global observations is 7 mm a^{-1}. However, Calais *et al.* (2003) suggest that Nubia–North America velocity has changed since 3 Ma, so that velocities averaged over longer periods may differ from the modern rate. Bonini *et al.* (1997) and Boccaletti *et al.* (1998, 1999) interpret the geometry and chemistry of volcanic deposits in the rift floor as further evidence for a change in the extension direction across the MER around the Pliocene–Quaternary boundary.

In contrast, relative velocities or opening rates calculated with local observations restricted to the length scale of the topographic rift (∼80–100 km in central Ethiopia) are smaller, from 2 mm a^{-1} using the volume of extruded Pliocene–Recent lava (Wolfenden *et al.* 2004) to 4 mm yr^{-1} (Bilham *et al.* 1999) from GPS observations between 1992 and 1997. The median opening rate of these local observations is 2 mm a^{-1}.

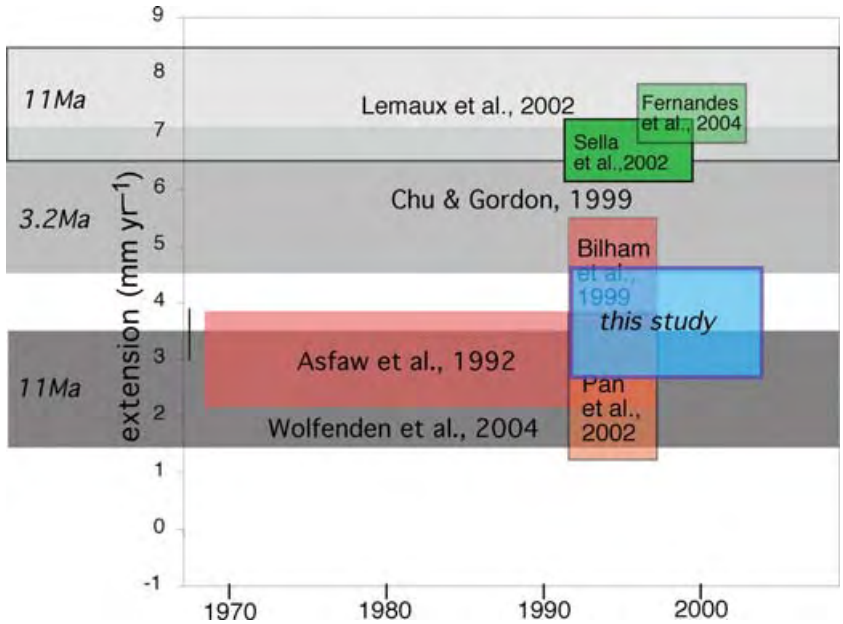

Figure 3. Estimates of relative Nubia–Somalia velocity from published sources as labelled (Asfaw *et al.* 1992; Chu & Gordon 1999; Bilham *et al.* 1999; Lemaux *et al.* 2002; Pan *et al.* 2002; Fernandes *et al.* 2004; Wolfenden *et al.* 2004). Light grey boxes are estimates from geology, and dark grey from seafloor spreading, with labels corresponding to approximate timescale, which exceeds the span of the x-axis. Green boxes are estimates from global GPS solutions; red are from campaign GPS, blue is the Nubia-fixed velocity estimated in this study. See text for discussion.

Discrepancy between observations of surface-relative velocity fields over different spatial scales is commonly used to constrain the apparent rigidity of an elastic crustal layer, expressed as the dislocation locking depth (e.g. Scholz 2002), with a positive correlation between rigidity (or elastic thickness) and the length scale of surface displacements (e.g. Burbank & Anderson 2001). Because the locally measured surface strain within the rift in central Ethiopia is less than the far-field estimated total strain budget, this reasoning suggests that the scale of strain accommodation in the African crust is greater than the width of the structural rift and therefore that the elastic rigidity of the crust is very large. Observations of near-surface heat flow (Huttrer 2001), seismic velocity (Keranen *et al.* 2004; Bastow *et al.* 2005), volcanism (Furman *et al.* 2006), seismic anisotropy (Keir *et al.* 2005) and structure (Ebinger *et al.* 1993) all preclude such a stiff crust; we hypothesize that the long length scale of the regional strain field is instead an artifact of the weakness of the crust in the MER, and that geodetic observations of regional surface displacements measure distributed deformation in a continuous, viscous lower crust beneath the rift. Any instantaneous elastic strain localization associated with seismicity and dike injection within the upper crust of the MER is rapidly dissipated in the lower crust because the elastic part of the crust is too weak to store large stresses for long times. Because the apertures of the geodetic and structural sections are comparable to the length scale over which strain is distributed, local estimates of opening underestimate the total relative motion between Nubia and Somalia.

In addition to distributing the surface displacement signal associated with rifting, viscoelastic crust should also undergo observable temporal variations in opening rate as strain localization events such as earthquakes or dike injections relax. Thatcher (1983) describes two models with equivalent temporal strain rate declines near a fault: thin lithosphere with stress relaxation accommodated by flow in the asthenosphere, or thick lithosphere with post-seismic creep on the deep portion of the fault plane. In either case, measurable decreases in local strain rate follow elastic failure events, and complicate the use of a strain budget in estimating recurrence intervals and long-term mean relative velocities. In all cases, the difference between 'weak' and 'strong' cases is not the absolute rigidity of the elastic layer, but whether failure occurs through the entire elastic layer or only in some part of it.

GEODETIC OBSERVATIONS OF RIFT OPENING

Laser ranging measurements accurate to 5 mm were first conducted in the MER in 1969 (Mohr 1974). These continued until 1976 and were ultimately combined with a subset of control points measured in 1992, 1995, 1997 and 2003 by GPS geodesy. The 1969–1992 extension rate was reported as 2.9 ± 1.6 mm yr^{-1} (1σ), although an apparent contraction in a laser-ranging line caused by the spurious motion of one control point led to an erroneous published cumulative rate estimate of 1.1 ± 2.2 mm yr^{-1} (Asfaw *et al.* 1992). Subsequent observations with GPS in 1995 and 1997 revealed a widening rate of 3.1 ± 0.9 (ADD1 to SELA) and 3.9 ± 0.9 mm yr^{-1} (ADD1 to BOLO) for the period 1992–1997 (Bilham *et al.* 1999). (See Fig. 2 for site locations.)

We measured a total of five surviving geodetic benchmarks spanning the central MER in 2003 January as part of the EAGLE project (Ethiopia-Afar Geoscientific Lithospheric Experiment) (Maguire *et al.* 2003). We combine these data with raw observations from GPS campaigns in 1992, 1995 and 1997. Site ADD1 (see Fig. 2) at the University of Addis Ababa Geophysical Observatory (UAAGO) served as the local base station, and logged data for 24 hr per day at 30-s intervals for the duration of all four GPS campaigns. In 1997, REDG also ran for the duration of the campaign, and ADD1 and REDG ran continuously for 5 months from 1997.5 to 1998.0 in order to measure regional tidal amplification (Bilham *et al.* 1999). All other stations ran for a minimum of 3 days during 18-hr sessions, logging data at 30-s intervals. REDG and BOLO are tied by simultaneous observations in 1997, and are treated as a single point called

Table 1. Geodetic site positions and velocities during 1992–2003.

Site	1992 epochs	1995	1997	2003	Longitude	Latitude	ITRF00 E (mm yr^{-1}) $\pm$ 1σ	ITRF00 N (mm yr^{-1}) $\pm$ 1σ	Nubia-fixed E (mm yr^{-1}) $\pm$ 1σ	Nubia-fixed N (mm yr^{-1}) $\pm$ 1σ
ADD1	015–029, 303–314	356–359	184–271	006–021	38.766	9.035	24.98 $\pm$ 0.6	16.64 $\pm$ 0.6	0.79 $\pm$ 0.6	$-$0.19 $\pm$ 0.6
KOLO	309–312	356–359	187–194		38.584	9.081	23.41 $\pm$ 1.1	16.47 $\pm$ 0.9	$-$0.77 $\pm$ 1.1	$-$0.4 $\pm$ 0.9
BOKU	027–028		191–193	012–017	39.282	8.472	27.24 $\pm$ 0.8	16.63 $\pm$ 0.7	3.09 $\pm$ 0.8	$-$0.11 $\pm$ 0.7
BOLO	306–308	356–359	192–199		39.52	8.258	28.07 $\pm$ 0.7	15.67 $\pm$ 0.6	3.93 $\pm$ 0.7	$-$1.05 $\pm$ 0.6
REDG			196–271	013–017	39.531	8.266	Tied to BOLO		Tied to BOLO	
GODE			206–209	019–021	43.568	5.931	24.91 $\pm$ 1	12.52 $\pm$ 0.8	0.92 $\pm$ 1	$-$3.49 $\pm$ 0.8

BOLO for all of the velocity and baseline solutions. The data epochs incorporated into the estimates of velocity presented here are given in Table 1.

Raw data from all observed epochs were processed at the University of Montana, using GAMIT/GLOBK (King & Bock 2000; Herring 2002). Velocity solutions in the ITRF00 reference frame (Table 1, Fig. 4a) were calculated by including the IGS global network in the calculation of regional site positions and velocities, and minimizing the departure of IGS reference sites from their reported positions and velocities in that reference frame. Only a relatively small number of global reference sites were available for the entire duration of this experiment starting in 1992. In addition, precise orbits were available beginning only in the end of 1992. Errors in position and velocity for the 1992 epochs are therefore significantly greater than those for later epochs; data are weighted according to uncertainty in the final velocity estimate. We also report velocities in an Nubia-fixed frame (Table 1, Fig. 4b), created by minimizing the velocities of campaign sites KOLO and ADD1 in addition to IGS sites located on the Nubian plate, including MAS1, SUTH, NKLG, ZAMB and YKRO. Of these sites, only the regional campaign sites have frame-defining observations for the entire duration of the experiment. In this Nubia-fixed frame, the southeastern rift shoulder (BOLO) moves at 4 $\pm$ 0.9 mm yr^{-1} (1σ) at 105°. This velocity is consistent with the rifting direction from structural analysis (Wolfenden *et al.* 2005) and the rate from previous geodetic observations (Bilham *et al.* 1999). Maximum strain is centred on BOKU, a geodetic monument located in the center of the rift valley, coincident with the closest active magmatic segment (Fig. 2). No strain localization occurs at either the northwest or southeast rift bounding faults. Gode (GOD1), near the Somali border, moves at 3.6 $\pm$ 1.3 mm yr^{-1} at 165° in the Nubia-fixed frame. The quality of this geodetic monument is dubious, as it is located on a cement slab on unconsolidated desert pavement.

In addition to regional station positions and velocities, we calculate a time-series of baseline length changes between two sites, ADD1 and BOLO, spanning the structural MER. ADD1 is located in Addis Ababa at the National Geophysical Observatory, on the northwestern rift shoulder. BOLO is located in the village of Bolo Mikael on the southeastern rift shoulder. Baseline length changes are direct observations of 1-D rift opening in the direction of the baseline (136°), independent of any reference frame considerations and of the GLOBK assumption of linear velocities. The mean linear

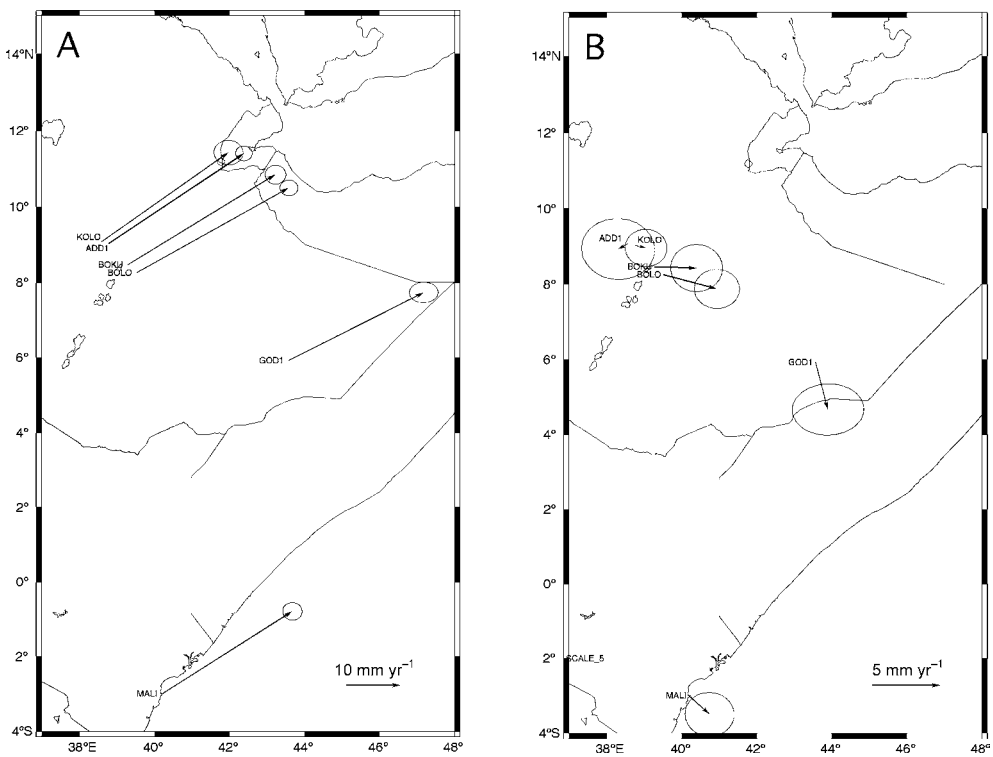

Figure 4. (a) Velocities of GPS sites measured in this experiment in the ITRF2000 reference frame. Error ellipses are 2σ. (b) Velocities in a Nubia-fixed frame, defined by minimizing the velocities of ADD1, KOLO and IGS sites on stable Nubia.

rate of baseline extension from this series, 3.3 ± 0.4 mm yr^{-1}, is equivalent to the Nubia-fixed velocity of BOLO projected onto the baseline, 3.5 ± 0.7 mm yr^{-1}. However, we observe that a constant linear velocity is a poor fit to the baseline length time-series. In the following sections, we interpret the secular variations in baseline-parallel velocity as the result of viscous relaxation of the rift following a dike injection event. We make no attempt to model seasonal variations in atmospheric conditions in either the velocity solutions or in the baseline time-series.

1993 STRIKE-SLIP FAULTING IN NAZRET

One potential source of secular variations in the rate of rift opening is a seismic event or series of seismic events near the geodetic baseline. Small local events recorded by the EAGLE network during 2002–2003 (Keir *et al.* 2006) within 1° of either the ADD1-BOLO or the ADD1-GODE baseline have a total moment of only 3.04 × 10^{14} N m, equivalent to a single Mw 3.6 event. Moment release occurs predominantly near the southeastern rift-bounding fault, with a smaller cluster of events in the centre of the rift. The surface displacement associated with these events is several orders of magnitude smaller than that detectable by a geodetic array. We therefore omit any consideration of microseismicity in the following model.

A Mw 5.3 strike-slip earthquake on 1993 February 13 is the sole teleseismic event in the region of the geodetic experiment. This event was relocated from the Harvard CMT epicentre by the UAAGO to 8.331°N, 39.308°E, 15 km from the ADD1-BOLO baseline, by combining five global catalogue observations of the main event with the locations of three foreshocks, the main event and an aftershock detected on three stations of the then active Ethiopian local network. The UAAGO also compiled eight local damage reports (Fig. 5).

We generate a forward model of surface displacement from this event using Coulomb 2.0 (Toda *et al.* 1998; King *et al.* 1994). We select the right lateral nodal plane of the Harvard CMT focal mechanism based on the distribution of recorded foreshocks and aftershocks in alignment with this plane (Fig. 5). Scaling of the failure surface and total slip are estimated from the reported scalar moment of 1.14 × 10^{17} N m, using empirical moment to length scaling relations (Scholz 2002). We model slip of 30 cm over a fault area of 5 × 10^{6} m^{2}, with the region of slip extending toward the geodetic baseline from the UAAGO epicentre in order to maximize displacement within the instrument array. The integrated dilatational strain from this dislocation produces an increase in the length of the ADD1-BOLO baseline of <0.1 mm, undetectable in geodetic observations. Surface displacements due to this event are highly non-unique, because we have no geometric constraints on the rupture plane other than the total moment and the absence of a surface rupture.

Fig. 6(a) shows maps of Coulomb stress at 5-km depth for opening of a vertical crack of strike 46° (normal to the geodetic baseline) produced by the 1993 rupture. A white bar shows the location of a continuously opening crack modelled by Bilham *et al.* (1999). Fig. 6(b) maps the Coulomb stress at 5 km for dextral slip on the 1993 failure plane (focal mechanism) produced by the instantaneous opening of a 1.5-m-wide dike at the location of a buried opening crack postulated by Bilham *et al.* (1999). We prefer to model the extensional event required by the geodetic observations as a single dike intrusion rather than a continuously opening crack, as discussed in the following section. Because the regional stress field is unconstrained in these models, the magnitude of Coulomb stresses

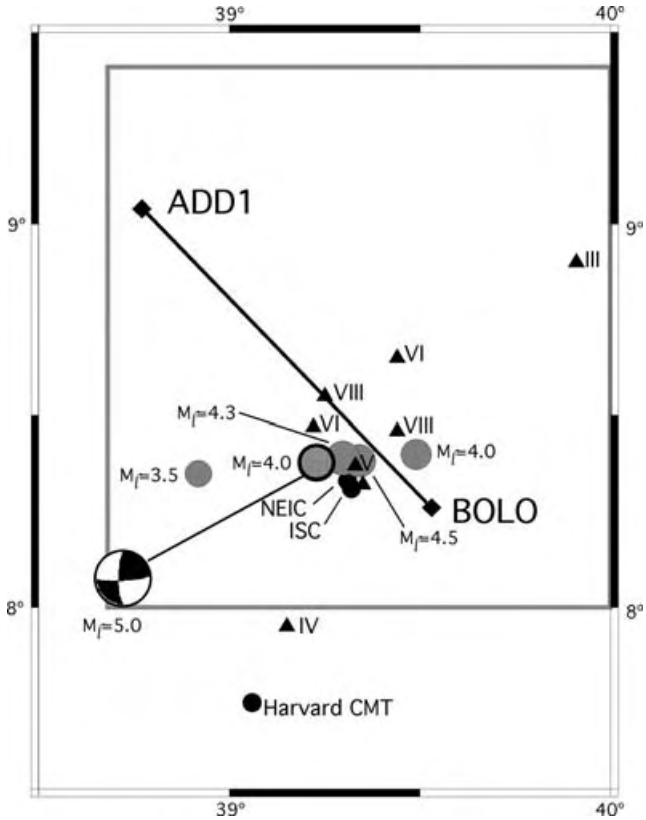

Figure 5. Observations of the 13 February 1993 Mw 5.3 strike-slip rupture. The epicentral location from the UAAGO is a black circle with the Harvard CMT solution shown. Foreshocks reported on a local network are grey; one recorded aftershock is hatched. Epicentral locations from global networks are black circles labelled with the network name. Triangles with adjacent Mercalli intensities locate villages with reported damage. The geodetic baseline is a solid line. The grey box shows the location of Fig. 6.

produced by these events is not significant. However, the sign of the stress changes allows us to conclude that the 1993 seismic event could have triggered the intrusion of a dike beneath the geodetic array, but the intrusion of a dike could not have triggered the 1993 strike-slip event. The dike is located entirely within a region of positive Coulomb stress produced by the 1993 event, suggesting that cracks in that region were encouraged towards failure after the earthquake. The 1993 rupture is in a region of negative Coulomb stress with respect to the dike, suggesting that dike intrusion would have impeded the 1993 rupture.

We draw two conclusions from the elastic models: (1) slip in the 1993 seismic event is insufficient to produce the observed displacement of geodetic markers, and (2) a dike injection event sufficient to produce the observed displacement could have been triggered by the 1993 event. In the following section, we model the surface displacements associated with a diking event located beneath the geodetic array, with temporal constraint imposed by the triggering hypothesis, such that dike injection is assumed to occur soon after 1993 February 13.

VISCOELASTIC MODELLING OF SURFACE DISPLACEMENT

We generate forward models of surface displacement along the geodetic baseline and at individual monuments as a function of time

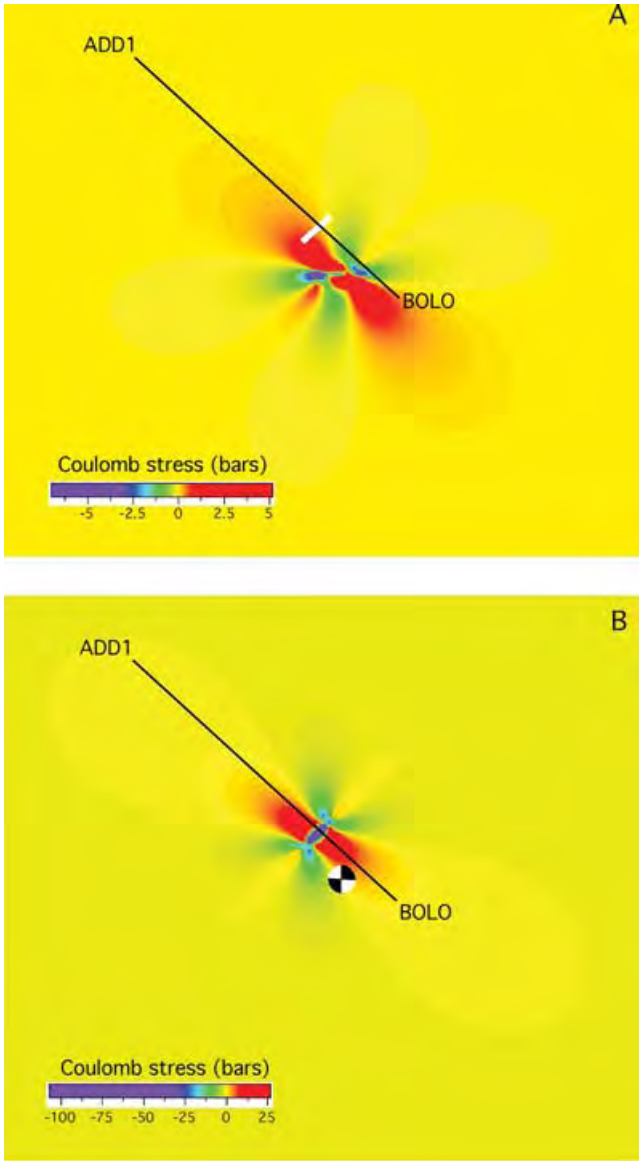

Figure 6. (a) Coulomb stress on a vertical opening crack of strike N46°E at 5-km depth produced by the 13 February 1993 strike-slip event. The location of the crack identified by Bilham *et al.* (1999) is given by a white bar. (b) Coulomb stress on a dextral fault of strike N89°E at 5-km depth produced by opening of a 1.5 m dike at the location reported in Bilham *et al.* (1999). The UAAGO location of the 13 February 1993 earthquake is marked with the CMT focal mechanism. Note that the magnitude of stress changes is not significant, but that faulting promotes diking while diking inhibits faulting. See text for discussion.

from a dike injection event immediately following the 1993 seismic event using Visco1D (Pollitz 1992). These solutions are calculated for a non-gravitating system of two layers: an elastic layer with moduli consistent with basalt composition, and a viscous half-space. We consider a range of viscosities in the half-space from 1.125×10^{18} Pa s to 1.125×10^{20} Pa s, corresponding to the range of viscosities for the asthenosphere estimated from postglacial rebound and post-seismic relaxation (Turcotte & Schubert 1982). We estimate solutions for models of end-member elastic thickness: 8 km from gravity admittance (Ebinger & Hayward 1996) or 15 km from seismogenic thickness (Maguire *et al.* 2006). We vary the geometry and size of the dike injection event, from a minimum volume event based on the widening estimate of Bilham *et al.* (1999) of 50 cm to a maximum widening of 2 m, through the entire elastic thickness of the model crust. A constraint of buried injection is imposed by the lack of reported surface volcanism in the period and location of interest. Bilham *et al.* (1999) require a depth of 3 km for their opening dislocation. However, we believe that their assumption of purely elastic deformation forces an unreasonable locking depth in order to reproduce the width of the strain field. Viscous flow at depth increases the wavelength of surface displacement allowing a shallower dislocation locking depth (upper limit of dike intrusion), and decreases the amplitude of the surface displacement, allowing more opening (a wider dike), to match the observed increase in baseline length.

End-member model results for baseline length over time are shown in Fig. 7. Models with 8 km elastic lids do not reproduce the duration of the opening observed on the geodetic array. Models with high viscosity ($\geq 10^{20}$ Pa s) in the viscous layer do not reproduce the amplitude of opening observed on the geodetic array given a reasonable dike width. The best fit to the observed displacement time-series is from injection of a 1.5 m dike at the position determined by Bilham *et al.* (1999) into a 15-km-thick elastic lid over a viscous layer of 1.125×10^{18} Pa s viscosity. Neither the spatial nor the temporal resolution of the GPS observations is sufficient to place constraints on the dike geometry, or resolve possible trade-offs among dike width, depth and crustal rheology. Instead, the modelling exercise described here is only intended to provide a conceptual explanation for the temporal variation in baseline strain rate we observe.

DISCUSSION

In summary, our study documents relative motion between Nubia and Somalia, as well as the mechanism by which this relative motion is locally accommodated in the region of the geodetic array. First, the total global extension between the stable Nubian and Somali plates is distributed over a horizontal length scale longer than the 80–100 km width of the structural MER. In a perfectly elastic system, a long length scale of deformation implies high rigidity, in conflict with a wide range of independent observations of rheology and thermal properties of the MER (e.g. Ebinger & Hayward 1996). We therefore draw the obverse conclusion: the distribution of relative motion between Nubia and Somalia implies that the MER is poorly described by elasticity. The high temperature and mechanical stretching associated with active rifting must force deformation into a viscous or viscoelastic regime, with a distributed continuous displacement field separating Nubia and Somalia, rather than a narrow, discrete, high-strain tectonic boundary. As with some other cases of continental deformation (e.g. Wright *et al.* 2004; Zhang *et al.* 2004), a combination of high strain rates and low elastic rigidity, causes the system to behave mechanically more like a continuous fluid than like a rigid elastic body. This end-member approximation of mechanical behaviour does not preclude episodic localized elastic failure, as tectonic forcing applies stress to even a thin elastic lid (Savage 1990).

Second, within the rift itself, extension is accommodated at least partially by aseismic dike injection. Diking is currently active and probably concentrated in the magmatic segments mapped by surface geology (Ebinger & Casey 2001) and seismic tomography (Keranen *et al.* 2004). Within the rift, a layer of apparent viscosity of 1.125×10^{18} Pa s is overlain by ~15 km of elastic material with the rheology of cold basalt. This elastic thickness is greater than that estimated

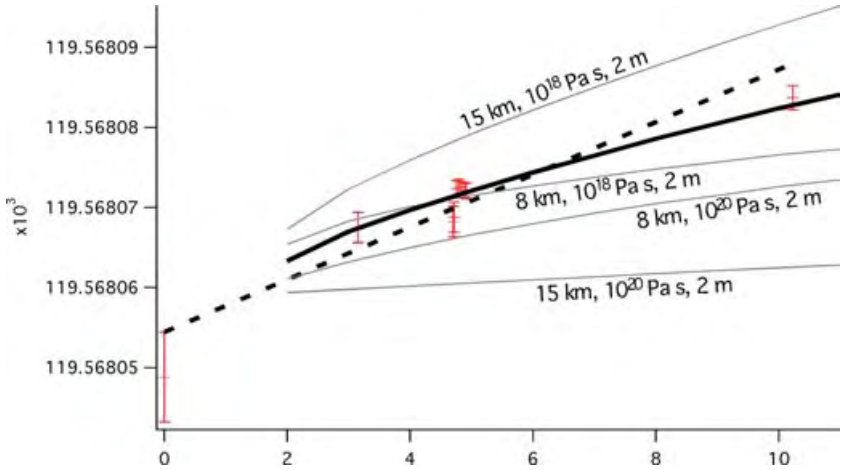

Figure 7. ADD1-BOLO baseline-length time-series and fits from viscoelastic models of surface deformation following hypothesized dike injection in 1993. The red markers are direct calculations of baseline length from GAMIT/GLOBK solutions, with 1σ error bars. Solid gray lines show the range of baseline behaviour for modelled viscoelastic crust. They are labeled with elastic thickness, viscosity of the viscous layer and dike width in that order. The dashed line is the best mean linear opening rate, 3.3 ± 0.4 mm yr^{-1}. The bold black line is the best viscoelastic model, showing injection of a 1.5-m wide dike into a 15-km thick elastic lid over a lower crust with viscosity of 1.125×10^{18} Pa s. For discussion see text.

from gravity admittance, as we might expect, since the timescale for flexure of the elastic crust under topographic loads is many orders of magnitude greater than the timescale of dike injection and subsequent crustal relaxation.

Dikes appear to intrude the elastic layer to very shallow depths without extrusion, possibly because they are narrow (here, ∼1.5 m) and therefore cool in tens of days. Diking processes also appear to be very quiet seismically, although few local seismic instruments were available at the hypothesized time of the event to record local microseismicity. Other recent observations suggest abundant microseismicity may occur during diking (Keir *et al.* 2004) thereby providing a target for future combined seismicity-geodesy campaigns. Dike injection may be triggered by local seismic failure, in this case the 1993 February 13, Mw = 5.3, earthquake. Opening of the MER does not occur by slip on rift-bounding normal faults.

Our interpretation of rifting processes depends on several significant assumptions that are exacerbated by the paucity of direct observations. The conclusion that relative motion between Nubia and Somalia is widely distributed is required by the results of many experiments showing the difference between local and regional extension rates (Fig. 3), and therefore is likely to be robust. The interpretation of secular rate changes in the rift itself is non-unique and poorly constrained, but in agreement with a hypothesis of magma-assisted rifting substantiated by considerations of seismic anisotropy (Gashawbeza *et al.* 2004; Kendall *et al.* 2005), surface structure (Ebinger & Casey 2001), upper mantle structure (Bastow *et al.* 2004, 2005), extrusion chemistry (Wolfenden *et al.* 2004; Furman *et al.* 2006) and fluid dynamics (Sleep 1997). The combined observations of distributed surface strain and secular changes in strain rate emphasize that viscous processes play a significant role in rifting of the African continent.

ACKNOWLEDGMENTS

The work in this paper was carried out with the support of NSF EAR grant 125968. 2003 data acquisition was part of the EAGLE project; NSF Continental Dynamics grant 0208475. Local seismic epicentres were provided by D. Keir and C. Ebinger, as were helpful comments. The lead author also wishes to acknowledge the field support of E. Gashaw and J. Khorsand. This is Cambridge Earth Sciences publication ES.8183.

REFERENCES

Acocella, V., Korme, T. & Salvini, F., 2003. Formation of normal faults along the axial zone of the Ethiopian Rift, *J. Structural Geol.,* **25,** 503–513.

Asfaw, L., Bilham, R., Jackson, M. & Mohr, P., 1992. Recent inactivity in the African rift, *Nature,* **357,** 447.

Bastow, I.D., Stuart, G.W., Kendall, J.-M. & Ebinger, C.J., 2005. Upper mantle seismic structure in a region of incipient continental break-up: Northern Ethiopian rift, *Geophys. J. Int.,* **162,** 479–493 doi: 10.1111/j.1365–246X.2005.02666.x, in press.

Bilham, R., Bendick, R., Larson, K., Mohr, P., Braun, J., Tesfaye, S. & Asfaw, L., 1999. Secular and tidal strain across the Main Ethiopian Rift, *Geophys. Res. Lett.,* **26,** 2789–2792.

Boccaletti, M., Bonini, M., Mazzuoli, R., Abebe, B., Piccardi, L. & Tortorici, L., 1998. Quaternary oblique extensional tectonics in the Ethiopian Rift (Horn of Africa), *Tectonophysics,* **287,** 97–116.

Boccaletti, M., Mazzuoli, R., Bonini, M., Trua, T. & Abebe, B., 1999. Plio-Quaternary volcanotectonic activity in the northern sector of the Main Ethiopian Rift: Relationships with oblique rifting, *J. African Earth Sci.,* **29,** 679–698.

Bonini, M., Souriot, T., Boccaletti, M. & Brun, J.-P., 1997. Successive orthogonal and oblique extension episodes in a rift zone: Laboratory experiments with application to the Ethiopian Rift, *Tectonics,* **16,** 347–362.

Burbank, D. & Anderson, R., 2001. *Tectonic geomorphology*, p. 274, Blackwell Science, Malden, MA.

Calais, E., DeMets, C. & Nocquet, J.-M., 2003. Evidence for a post-3.16-Ma change in Nubia-Eurasia-North America plate motions? *Earth planet. Sci. Lett.,* **6825,** 1–12.

Chu, D. & Gordon, R., 1999. Evidence for motion between Nubia and Somalia along the Southwest Indian ridge, *Nature,* **398,** 64–67.

Ebinger, C. & Casey, M., 2001. Continental breakup in magmatic provinces: An Ethiopian example, *Geology,* **29,** 527–530.

Ebinger, C. & Hayward, N., 1996. Soft plates and hot spots: Views from Afar, *J. geophys. Res.,* **101,** 21 859–21 876.

Ebinger, C., Yemane, T., Woldegabriel, G., Aronson, J. & Walter, R., 1993, Late Eocene-Recent volcanism and faulting in the southern main Ethiopian rift, *J. geol. Soc. Lond.,* **150,** 99–108.

Engdahl, E., van der Hilst, R. & Buland, R., 1998. Global teleseismic earthquake relocation with improved travel times and procedures for depth determination. *Bull. seism. Soc. Am.,* **88,** 722–743.

Fernandes, R., Ambrosius, B., Noomen, R., Bastos, L., Combrinck, L., Miranda, J. & Spakman, W., 2004. Angular velocities of Nubia and Somalia from continuous GPS data: Implications on present-day relative kinematics. *Earth planet. Sci. Lett.,* **222,** 197–208.

Foster, A. & Jackson, J., 1998. Source parameters of large African earthquakes; implications for crustal rheology and regional kinematics, *Geophys. J. Int.,* **134,** 422–448.

Furman, T., Bryce, J., Rooney, T., Hanan, B., Yirgu, G. & Ayalew, D., 2005, Heads and tails: 30 My of the Afar plume, in *Structure and evolution of the East African Rift System in the Afar Volcanic Province*, eds Yirgu, G., Ebinger, C.J. & Maguire, P.K.H., Geol. Soc. Lond. Spec. Pub., **259,** 97–121.

Gashawbeza, E.M., Klemperer, S.L., Nyblade, A.A., Walker, K.T. & Keranen, K.M., 2004. Shear-wave splitting in Ethiopia: Precambrian mantle anisotropy locally modified by Neogene rifting. *Geophys. Res. Lett.,* **31,** L18602, doi:10.1029/2004GL020471.

Gloaguen, R., Kurz, T., Ebinger, C., Casey, M. & Abebe, B., 2003. Atypical normal fault morphology in the Main Ethiopian Rift, *(abstract) EOS, Trans. Am. geophys. Un.,* **84,** Fall Meet. Suppl., S51C-0072.

Herring, T., 2002. *GLOBK: Global Kalman Filter VLBI and GPS Analysis Program Version 10.0*, Massachusetts Institute of Technology, Cambridge.

Hofstetter, R. & Beyth, M., 2003. The Afar Depression: Interpretation of the 1960–2000 earthquakes, *Geophys. J. Int.,* **155,** 715–732.

Huttrer, G., 2001. The status of world geothermal power generation 1995–2000, *Geothermics,* **30,** 1–27.

Kebede, F. & Kulhanek, O., 1991. Recent seismicity of the East African Rift system and its implications, *Phys. Earth planet. Int.,* **68,** 259–273.

Keir, D., Ebinger, C., Stuart, G., Daly, E. & Ayele, A., 2004. Seismicity of the northern Main Ethiopian rift, in *Proceedings of the International Conference on the East African Rift System, June 20–24 2004,* pp. 93–96, eds Yirgu, G., Ebinger, C. & Mulugeta, G., Ethiopian Geosci. Mineral Engin. Assoc., Addis Ababa, Ethiopia.

Keir, D., Ebinger, C., Stuart, G., Daly, E. & Ayele, A., 2004. Strain accommodation by magmatism and faulting at continental breakup: Seismicity of the northern Ethiopian rift, *J. geophys. Res.*, in press.

Keir, D., Kendall, J., Ebinger, C. & Stuart, G., 2005. Variations in late syn-rift melt alignment inferred from shear-wave splitting in crustal earthquakes beneath the Ethiopian rift, *Geophys. Res. Lett.,* **32,** L23308: doi 10.1029/2005/GL024150.

Kendall, J., Stuart, G., Ebinger, C., Bastow, I. & Keir, D., 2005. Magma-assisted rifting in Ethiopia, *Nature,* **433,** 146–148.

Keranen, K., Klemperer, S., Gloaguen, R. & EAGLE working group, 2004. Three-dimensional seismic imaging of a protoridge axis in the Main Ethiopian rift, *Geology,* **32,** 949–942.

King, R. & Bock, Y., 2000. Documentation for the GAMIT GPS Analysis software, version 10.0. Massachusetts Institute of Technology, Cambridge.

King, G., Stein, R. & Lin, J., 1994. Static stress changes and the triggering of earthquakes, *Bull. seism. Soc. Am.,* **84,** 935–953.

Knox, R., Nyblade, A. & Langston, C., 1999. Upper mantle S velocities beneath Afar and western Saudi Arabia from Rayleigh wave dispersion, *Geophys. Res. Lett.,* **25,** 4233–4236.

Lemaux, J., Gordon, R. & Royer, J-Y., 2002. Location of the Nubia-Somalia boundary along the Southwest Indian Ridge, *Geology,* **30,** 339–342.

Maguire, P.K.H. *et al.*, 2003. Geophysical project in ethiopia studies continental breakup, *EOS, Trans. Am. geophys. Un.,* **84,** 342–343.

Maguire, P.K.H. *et al.*, 2006. Crustal structure of the northern main Ethiopian rift from the EAGLE controlled source survey; a snapshot of incipient lithospheric break-up, in *Structure and Evolution of the East African Rift System in the Afar Volcanic ProvinceThe East African Rift System: Dynamics, Evolution and Resources*, eds Yirgu, G., Ebinger, C.J. & Maguire, P.K.H., Geol. Soc. Lond. Spec. Pub., **259,** 271–293.

Mohr, P., 1974. Ethiopian Rift geodimeter survey, *Smithsonian Astr. Obs. Special Report,* **376,** 111.

Pan, M., Sjoeberg, L.E., Asfaw, L.M., Asenjo, E., Alemu, A. & Hunegnaw, A., 2002. An analysis of the Ethiopian Rift Valley GPS campaigns in 1994 and 1999, *J. Geodyn.,* **33,** 333–343.

Pollitz, F., 1992. Postseismic relaxation theory on the spherical earth, *Bull. seism. Soc. Am.,* **82,** 422–453.

Savage, J. & Prescott, W., 1978. Asthenosphere readjustment and the earthquake cycle, *J. geophys. Res.,* **83,** 3369–3376.

Scholz, C., 2002. *The Mechanics of Earthquakes and Faulting*, 2nd ed. pp. 97–159, Cambridge University Press, Cambridge, UK.

Sella, G., Dixon, T. & Mao, A., 2002. REVEL: A model for Recent plate velocities from space geodesy, *J. geophys. Res.*, **107,** doi:10.1029/2000JB000033.

Sleep, N., 1997. Lateral flow and ponding of starting plume material, *J. geophys. Res.,* **102,** 10 001–10 012.

Thatcher, W., 1983. Nonlinear strain buildup and the earthquake cycle on the San Andreas Fault, *J. geophys. Res.,* **88,** 5893–5902.

Toda, S., Stein, R., Reasenberg, P. & Dieterich, J., 1998. Stress transferred by the Mw-6.5 Kobe, Japan, shock: Effect on aftershocks and future earthquake probabilities, *J. geophys. Res.,* **103,** 24 543–24 565.

Turcotte, D. & Schubert, G., 1982. *Geodynamics*, p. 450 pages. John Wiley and Sons, New York.

Weeraratne, D.S., Solomon, S.C. & Nyblade, A.A., 2005. Lithospheric deformation beneath the ethiopian plateau, *EOS, Trans. Am. geophys. Un.*, Fall Meeting Volume, T522B-07.

Woldegabriel, G., Aronson, J. & Walter, R., 1990. Geology, geochronology, and rift basin development in the central sector of the Main Ethiopia Rift, *Geol. soc. Am. Bull.,* **102,** 439–458.

Wolfenden, E., Ebinger, C., Yirgu, G., Deino, A. & Ayalew, D., 2004. Evolution of the northern Main Ethiopian rift: Birth of a triple junction, *Earth planet. Sci. Lett.,* **224,** 213–228.

Wolfenden, E., Ebinger, C., Yirgu, G., Renne, P.R. & Kelley, S.P., 2005. Evolution of a volcanic rifted margin: Southern Red Sea, Ethiopia. the southern Red Sea rift: Birth of a magmatic margin, *Bull. geol. Soc. Am.,* **117,** 846–864.

Wright, T., Parsons, B., England, P. & Fielding, E., 2004. InSAR observations of low slip rates on the major faults of Western Tibet., *Science,* **305,** 236–239.

Zhang, P. *et al.*, 2004. Continuous deformation of the Tibetan Plteau from Global Positioning System data, *Geology,* **32,** 809–812.